and what Ainleyet al. [2003] meant by "passive" interference); and (iii) interference competition by seabirds avoiding each other in some way or contesting access to food behaviorally ("direct" interference). The latter is not considered in any of the previous papers, but it is a logical possibility.

A fourth mechanism is suggested by considering that, in the model of Lewis et al. (2001), neither birds nor prey are strategic agents that can make decisions. An extensive literature now considers "the ecology of fear" (e.g. Brown 2007) and shows that prey can strategically avoid areas of high predation risk without necessarily having to be "disturbed" by predators. For example, Antarctic penguins alter their foraging behavior during darkness, i.e. refrain from entering the water, because it is more dangerous (Ainley & Ballard 2012, and references therein).

So far as we are aware, the only studies that have formally considered, based on knowledge about seabirds and their prey, how underlying processes might combine to create the halo are those of Lewis et al. (2001), Ainleyet al. (2003) and Gaston et al. (2007; see above). Gaston et al. (2007) calculated the relative availability

The maximum distance from the island (with radius r) to whichand (iii) fish biomass growth and depredation (Fig. 2). At the birds and fish can move is divided into s (= 25 in our model) rings of equal width Δs(Fig. 1). The area of the jth ring is

$$A_j = \pi(r + j\Delta s)^2 - \pi(r + (j - 1)\Delta s)^2 \text{ for } j = 1,2 \ldots, s$$

and thus the surface area of successively more distant rings is larger. We model the distributions of birds and fish over these rings. When referring to fish and bird density, upper case F and B are used, while absolute biomass of fish and number of birds are denoted with lower case f and b.

Each model run consisted of 810 iterations (representing 2 h time steps over 90 d). In each time step, three calculations are made, in the following order: (i) bird redistribution, (ii) fish redistribution

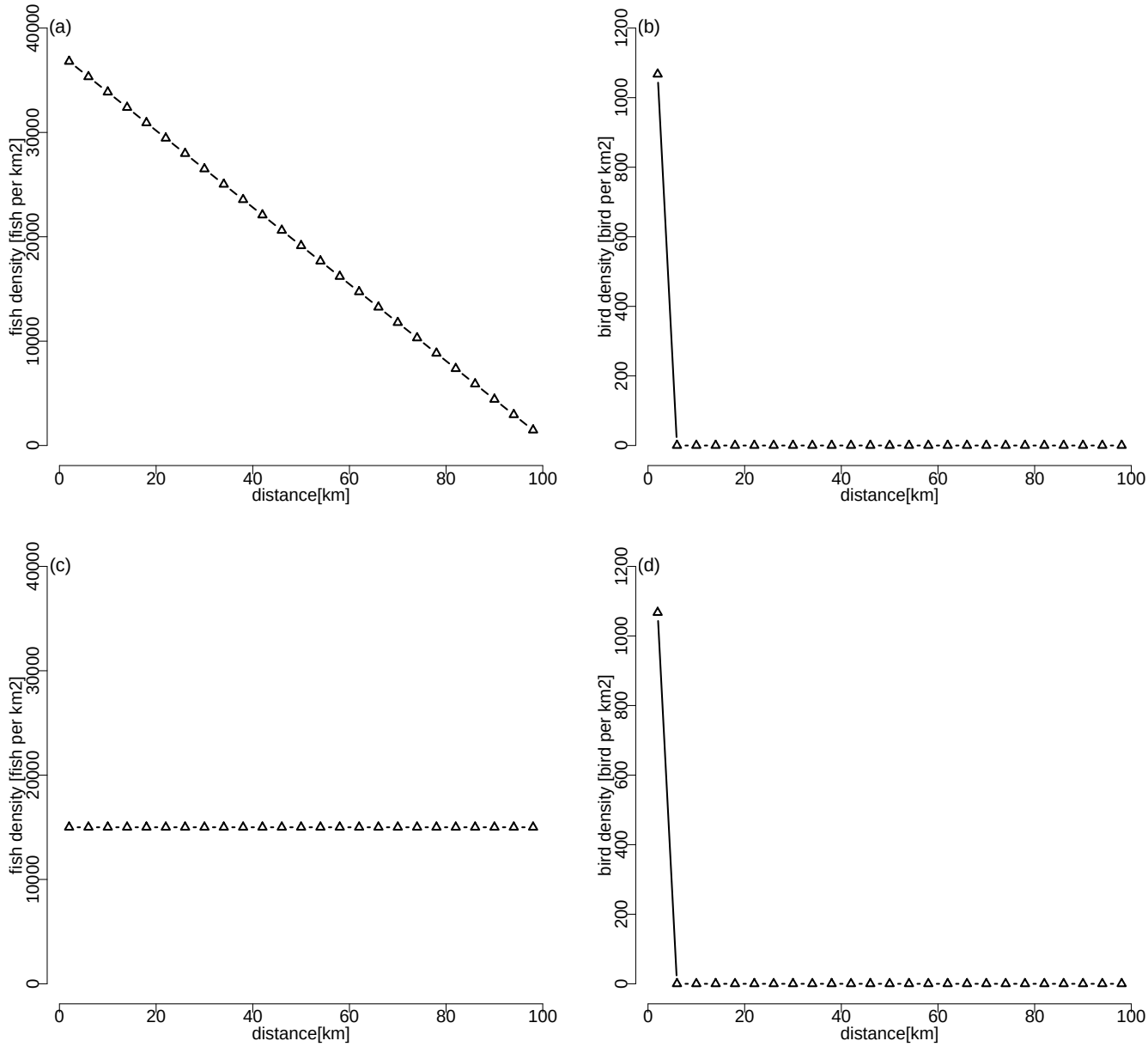

Fig. 3. Initial fish density (left panels a and c) and initial bird density (right panels b and d) as function of distance from the island, in the cases in which (upper panels) the input rate of food for fish is strongest close to the island (upwelling), and (lower panels) the input rate of food for fish is equal across the foraging range.

Predation by seabirds takes place after redistribution of fish, using updated fish densities $F_j(n + 1)$ (= $f_j(n + 1)/A_j$).

Parameterization

All parameters, their description and their default values are listed in Table 1. These values are not intended to represent particular species, but to represent a general situation.

Analysis

The aim of our analysis is to compare the development and shape of Ashmole's halo between the two basic scenarios in which (a) fish diffuse (random behavior), or (b) in which fish are strategists that exhibit fitness-maximization behavior. We compare these using the default parameter set. To provide a sensitivity analysis, we randomly drew 100 combinations of parameter values

TABLE 1
Parameters and state variables of a model of Ashmole's halo

	Parameter	Description	Unit	Value
a	A_j	area of site j	km^2	$\pi((r+j)^2-(r+j-1)^2)$
	b_{ini}	initial number of birds (1 per 1000 kg fish)	–	15
	D	diffusion coefficient	$km^2\ h^{-1}$	1.2
	d_j	distance of midpoint of site j to the island	km	$(j-0.5)\ \Delta s$
	f_{ini}	initial biomass of fish	kg	15 000
	Δn	duration of time step	h	2
	Δs	width of each ring around the island	km	0.08
	h	hunting capacity	$km^2\ h^{-1}$	0.0001
	m_n	natural death	h^{-1}	1/21 900
	N	number of time steps (for 90 days)	–	1 080
	p_b	proportion of birds taking a decision each time step	–	0.1
	p_f	proportion of fish taking a decision each time step	–	0.75
	r	radius of the island	km	24
	s	total number of sites	–	25
	$s\cdot\Delta s$	maximum distance birds and fish can dwell	km	4
	$t_{t,j}$	travel time for return trip to site j	h	$2\ d_j/v$
	u_{max}	fish biomass increase per time step of site with maximum food availability (first site)	$kg\ h^{-1}\ km^{-2}$	10
	v	flight velocity	$km\ h^{-1}$	60
	State variable	Description		
b	$b_{e,j}(n)$	number of birds emigrating from site j at time step n		
	$b_j(n)$	number of birds in site j at time step n		
	$f_{e,j}(n)$	fish biomass emigrating from site j at time step n		
	$f_j(n)$	fish biomass in site j at time step n		
	$F_j(n)$	density of fish in site j at time step n		
	$g_j(n)$	gain per fish in site j at time step n		
	$m_j(n)$	site-specific mortality rate in site j at time step n		
	$q_{f,j}(n)$	quality of site j from fish's perspective		
	$q_{b,j}(n)$	quality of site j from bird's perspective		
	$t_{h,j}(n)$	site-specific hunting time in site j at time step n		
	$u_j(n)$	upwelling rate of food per area in site j at time step n		

from uniform distributions between a minimum and maximum fitness-maximization simulation runs. We examined the resulting value (Table 2), and compared the outcomes of random and distributions for differences in shape.

TABLE 2
Default values and variation range of parameters varied in the pairwise comparison

Parameter	Meaning	Default value	Minimum	Maximum
v	flight velocity	60	30	90
h	hunting capacities	0.0001	0.00005	0.00015
u_{max}	fish biomass increase per time step of site with maximum food availability (first site)	10	5	15
m_h	natural death	2/(24 × 5 × 365)	2/(24 × 8 × 365)	2/(24 × 2 × 365)
D	diffusion coefficient	1.2	0.2	2
r_{bf}	number of birds per kg fish biomass	0.001	0.0005	0.0015

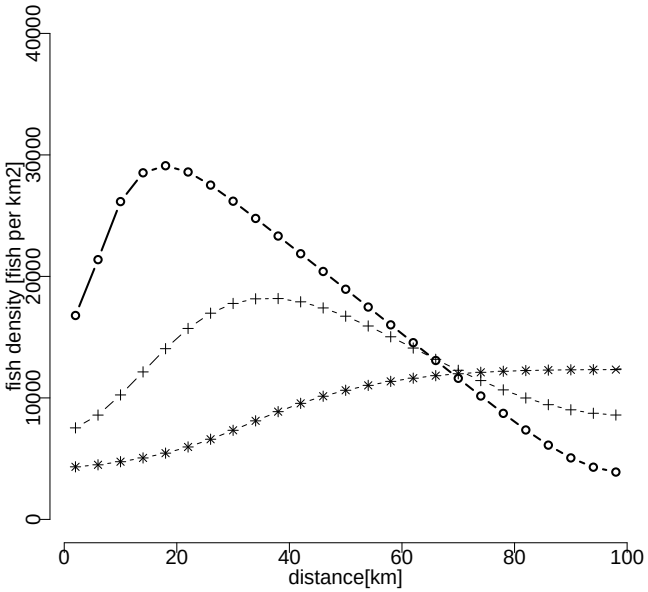

Fig. 4. The development of prey and predator distributions when fish movement is random, shown after various time periods (see key on graphs). Fish densities (left panels a and c) and bird densities (right panels b and d) are shown as function of distance from the island, in the cases in which (upper panels) the input rate of food for fish is strongest close to the island, and (lower panels) the input rate of food for fish is equal across the foraging range.

Predictions

We expected (i) that the halo would be deeper and larger when fitness-maximization behavior of fish is included, (ii) that the halo would develop more rapidly when the fish exhibit fitness-maximization behavior, and (iii) that the fish stock will decrease less with fitness-maximization behavior than when they move randomly.

RESULTS

Random behavior

Starting from the initial fish and bird density distributions shown in Figure 3, we show in Figure 4 the progression of fish and seabird distributions as iterations proceed, assuming random fish redistribution. The development of the bird distribution is very similar whether there is upwelling (Fig. 4b) or not (Fig. 4d). With upwelling, the fish distribution initially increases strongly with distance from the island, but flattens and acquires the sigmoidal shape typical of diffusion processes by iteration 360 (~ day 30). If diffusion were the only process taking place, the equilibrium density of fish would eventually be equal everywhere, but here predation and growth give the distribution its shape, with the furthest sites eventually having the highest fish density. With no upwelling, the halo starts to develop immediately, because fish started out with equal densities throughout the considered region. By day 90, the shape of the halo is similar with and without upwelling.

Table 2. We investigated how often four basic features developed in the 100 simulations, and compared the outcomes between random and fitness-maximization simulation runs. The four basic features are shown in Figure 7. They are:

Feature 1 Bird density drops off steeply after the first site.

Feature 2 Bird density increases over part of the foraging range (i.e. has a hump).

Feature 3 Bird density is high close to the island, and falls abruptly to zero partway through the foraging range.

Feature 4 The highest fish density co-occurs with the maximum range that birds use, and thereafter falls.

We considered the robustness of these differences between random and adaptive fish movement by investigating how often these features were present in the 100 simulations with randomly drawn parameters. We report the results for randomization and fitness maximization, after 360 iteration steps and after 980 iteration steps.

Feature 1 In all cases, under both randomization and fitness-maximization, the first site had the highest bird density. However, the decrease from the first to the second

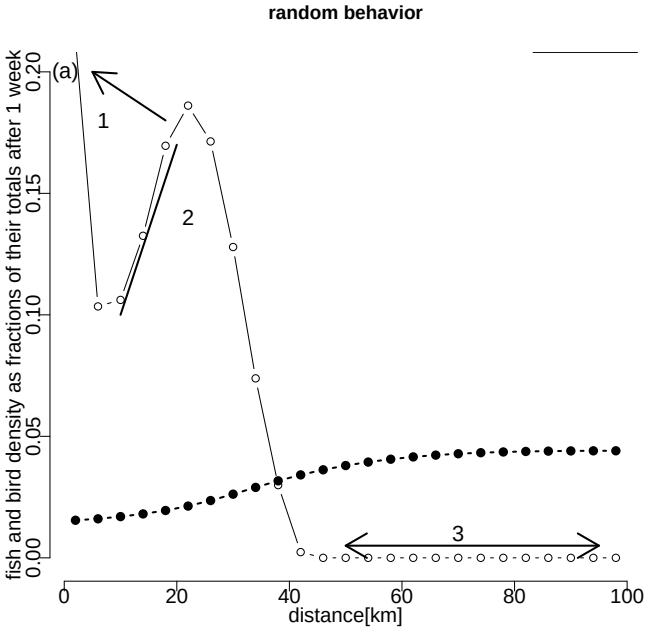

Fig. 7. Basic features of the distributions of fish and seabirds emerging after 360 iterations for the four scenarios. The numerals 1 to 4 indicate these features, which are discussed in the main text. Panels (a and c) show random behavior and panels (b and d) fitness-maximizing behavio In the upper panels, the input rate of food for fish is strongest close to the island (upwelling), and in the lower panels, the input rate of food for fish is equal across the foraging range. The total input over the area is equal in both cases. Densities have been rescaled for portrayal.

site is abrupt under random fish movement, and much smoother under fish fitness-maximization.

Feature 2 Under randomization, a hump in the bird density was present in 97 out of 100 simulations at 360 iterations. The three cases lacking a hump were those with a high diffusion co-efficient and low flight speed. The hump later appeared in these three simulations and was present at 1080 iteration steps. Under fitness-maximization, in contrast, there were only nine simulations that displayed any sort of a hump somewhere along the bird distribution. In all cases, the hump was very small and the effect can likely be ascribed to local instability.

Feature 3 Under fitness-maximization, birds always range to the maximum distance (site 25; occasionally numbers are very low), but when fish exhibit random behavior, birds do not range nearly this far, reaching on average to site 12 after 360 iteration steps and site 14 after 1080 iteration steps. Both fish and birds are distributed further out when the fish exhibit fitness-

Feature 4 Under random behavior, the highest fish density is further out than the maximum bird range in 93 out of 100 simulations at 360 iteration steps, and 100 out of 100 simulations at 1080 iteration steps. Under fitness-maximization this never occurs. When the fish conduct random behavior, the birds on average do not go out further than site 13 or 14, whereas the fish density is still increasing from that point on.

The appearance of these four features without upwelling (lower panels, Fig. 7) is nearly identical, the sole exception being that with upwelling there is a sharp drop-off in fish density at the far end of the foraging range (Fig. 7b), while this does not occur when food input is equal across the foraging range (Fig. 7d). With fitness-maximization, birds range much further than under random fish movement, the halo is deeper and stronger, and these features do not appear sensitive to the parameter values chosen under any of the four basic scenarios.

Halo development

Using the default parameter set, the halo develops much more quickly when fish exhibit fitness-maximizing behavior than when they move randomly. Figures 8a,c show the distribution of fish after 23 (~2d) iterations, as well as (Fig. 8b,d) the course of events at the second site. This comparison also reveals that the change is smoother when fish move randomly. Under fitness-maximization, instability is evident, although it is small enough not to disturb the general pattern.

Fish population dynamics

The fish population declines more quickly when the fish move randomly than when they make fitness-maximizing movements. When moving randomly, on average 70% of fish are still alive after 360 iterations and 53% after 1080 iterations, while the equivalent figures under fitness-maximization are 91% and 78%.

DISCUSSION

Our results show that Ashmole's halo develops more deeply and quickly around a seabird colony when prey have the capability of responding to the presence of seabirds by moving adaptively (i.e. to increase fitness) rather than by moving randomly. Our sensitivity analysis further suggests that this is a robust conclusion, not strongly dependent on any of the parameter values. Previously, Gaston et al. (2007) showed theoretically that Ashmole's halo develops under a broad range of conditions even if prey did not move. Here, we found that without any adaptive movement the fish population was reduced by 53%, but with adaptive movement it was reduced by only 22%. While these quantities obviously depend on the parameter values and simulation procedure, the effect of adaptive movement is clearly significant and strengthens the halo effect, although fewer fish are consumed by the predators. Our results suggest that the phenomenon is as profound as Ashmole (1963) originally surmised, and so able to affect seabird life histories.

The only other direct analyses of Ashmole's halo are those of Lewis et al. (2001) and Ainley et al. (2003). Their model assumes that prey respond to disturbance from predators either by swimming away or by moving deeper; in either case, their availability to predators is temporarily reduced. Ainley et al. (2003) showed that, in fact, fewer herring schools Clupea harengus are found at the surface where surface-foraging kittiwakes are intensively foraging, as a function of proximity to the colony. The fitness-maximizing version of the model developed here in effect assumes that prey assess the "danger" level (i.e. the mortality rate that they would experience if they undertook no predator evasion; see Lank & Ydenberg 2003) and respond accordingly: no direct encounter with a predator is required — although, of course, such encounters would inform their estimate of the danger. Our model makes no specific assumptions about how the information is acquired, but a variety of sources are possible, including the behavior of conspecifics.

Although the details of the competitive mechanism are slightly different, both the model of Lewis et al. (2001) and that presented here develop halos around seabird colonies. The halo in our model develops quickly, while Lewis et al. (2001) state that when fish respond by lateral swimming "a slowly growing halo is readily generated." However, model details are sufficiently different that the meaning of "quick" versus "slow" is not at all clear. Lewis et al. (2001) add "that factors such as currents or disturbance by other predatory species may effectively mix shoals to such an extent that halo patterns do not form clearly." (For example, the arrival of foraging whales increases trip length, i.e. halo size, in penguins; Ainley et al. 2006.) Lewis et al. (2001) claim that, because each seabird requires approximately the same total area to obtain food, independent of colony size, their basic result (trip time increases as the square root of colony size) holds. However, their brief presentation of results does not include many details.

One possibility that might affect halo development is whether prey are benthic or schooling fish. The study of Birt et al. (1987), one of only three that have directly measured a halo, concerned benthic fish; the study by Ainley et al. (2003) concerned schooling, pelagic fish. It seems likely that both types of prey would have behavioral mechanisms that reduce their availability to predators, but these are likely to be rather different (e.g. hiding versus fleeing) and so would affect halo development.

When prey as well as predators are strategic agents, their interaction should be considered in an evolutionary game theoretical context (Nowak & Sigmund 2004). In a predator-prey game, the decisions of individual prey depend not only on those of other prey, but also on decisions made by predators, and vice versa. Although there are intellectual predecessors, the first paper that explicitly formulated predator-prey interactions as a predator-prey game was that of Sih (1994; see also Sih 1998). Subsequent investigations have applied predator-prey game models to specific systems such as desert rodents facing snakes, foxes and owls (Bouskila 2001, Kotler et al. 2002), Antarctic krill Euphausia superba and penguins (Alonzo et al. 2003), and tadpoles and dragonflies (Hammond et al. (2007).

The basic concept of the spatial game modeled here is the "ideal free" distribution (IFD; Milinski & Parker 1991). When sites have associated predation danger in addition to food availability, fitness at equilibrium is equalized as in the basic IFD model, with fitness having both resource-gain and survival components (Grand 2002). But because the level of predation danger at any site depends on the behavior of the predators themselves, the distribution game of both prey and predators must be considered. Predator-prey gaming models retain the essential properties of the IFD in that, at equilibrium, no individual can benefit from (unilaterally) moving to

a different site (Nash equilibrium). Some models also demonstrate that the equilibrium is stable to invasion by initially rare alternative tactics (an evolutionary stable strategy or ESS; technical details and exact definitions in Houston & MacNamara 1999). Our model suggests that the basic properties of Ashmole's halo arise in a predator-prey game.

The most straightforward way to test these ideas would be to estimate in a field situation the contributions of prey depletion and the anti-predator behavior of the prey to the delivery rate achieved by provisioning seabirds. For example, prey density might be reduced